NANOSTRUCTURED FLUIDS FOR THE SELECTIVE REMOVAL OF A NON-ORIGINAL VARNISH FROM A 20th CENTURY OIL PAINTING AT THE PEGGY GUGGENHEIM COLLECTION, VENICE

Luciano Pensabene Buemi[a*], Maria Laura Petruzzellis[a], David Chelazzi[b], Michele Baglioni[b@], Rosangela Mastrangelo[b], Rodorico Giorgi[b], Piero Baglioni[b@*]

[a]Conservation Department, Peggy Guggenheim Collection, Venice, Italy.

[b]Consorzio Interuniversitario per lo Sviluppo dei Sistemi a Grande Interfase (Center for Colloid and Surface Science), CSGI, and Chemistry Department, University of Florence, Via della Lastruccia 3, Sesto Fiorentino, 50019 Florence, Italy.

*Corresponding author: Piero Baglioni: piero.baglioni@unifi.it; Luciano Pensabene Buemi: lpensabene@guggenheim-venice.it

Abstract

This paper reports on the evaluation of a polyvinyl alcohol (PVA) "twin-chain" polymer network (TC-PN) combined with an oil-in-water nanostructured fluid (NSF) for the removal of a polyvinyl acetate (PVAc) varnish. Small Angle X-ray Scattering, Confocal Laser Scanning Microscopy, and Fluorescence Correlation Spectroscopy showed that the structure of the gel and the NSF are only minimally altered by loading the fluid into the gel. The NSF is partially free to diffuse through the network, but also interacts with the gel walls. During the cleaning, the dynamics of the fluid at the gel-substrate interface are controlled by the osmotic balance taking place among the interconnected pores. These features grant effective and controlled cleaning performances.
The case study identified for this research is Pablo Picasso's *The Studio* (*L'Atelier*, 1928), one of the masterpieces in the Peggy Guggenheim Collection, Venice (PGC). In 1969 the oil painting, originally unprotected, was wax-lined and then varnished using a PVAc varnish. Over the years, the white shades of the painting have been compromised by the yellowing of the varnish and soiling of deposits. On painting mock-ups, the NSF-loaded hydrogels allowed the swelling and softening of PVAc varnish and wax layers, which were then removed with gentle mechanical action. Effective varnish and wax removal at the micron scale, and the absence of residues from the cleaning system (gel and NSF), were confirmed by Fourier Transform Infrared Spectroscopy (FTIR) 2D imaging. The effective and safe removal of the aged PVAc varnish and wax layer from the surface of the painting was then carried out using the same cleaning protocol successfully tested on the mock-ups, setting the NSF-loaded PVA TC-PNs as robust and reliable tools for the cleaning of sensitive works of art.

INTRODUCTION

Over the last three decades, research increased our knowledge of the chemical, physical and mechanical properties of modern paints, and of their behavior and ageing over time. However, their conservation is still an open issue. The PGC took part in the Nanorestart project funded by the European Union to evaluate novel nanostructured complex fluids and gel systems for cleaning the sen-

sitive surfaces of modern and contemporary paintings. The research focused on the removal of grime and dirt from unvarnished and complex surfaces, and the removal of unauthentic coatings from modern oil paints. Some issues have been identified as the occasion for ethical, theoretical, scientific and practical in-depth study. The triennial project involved selected case studies from the collection of the PGC: Jackson Pollock, *Two* (1943-45), and *Eyes in the Heat* (1946-47); Pablo Picasso, *The Studio* (1928); Giorgio de Chirico, *The Gentle Afternoon* (1916). These served as exemplary studies of the many conservation issues addressed by research, given the specific needs of each work of art.

The teamwork by conservators and scientists and their accurate assessment allowed the validation of PVA-based hydrogels, developed by Consorzio Interuniversitario per lo Sviluppo dei Sistemi a Grande Interfase (CSGI), and made of polyvinyl alcohol chains (PVA) combined with PVA of lower molecular weight. These "twin-chain" polymer networks (TC-PNs) proved to be advantageous systems for the cleaning of paintings, owing to their mechanical properties, retentiveness, ability to remove soil, and the safeness of the cleaning process. The TC-PNs were used for the first time to confine aqueous solutions and remove dust and dirt from the two aforementioned works by Pollock [1], as part of a conservation program on the eleven works by Pollock at the PGC (for overview of the program https://www.guggenheim-venice.it/en/art/conservation/case-studies/pollock/). The TC-PN used on the Pollock paintings had a unique formulation in order to adapt to the specific requirements of those works, but served as a prototype for a series of multipurpose gels, which were formulated to target typical cleaning cases and named Nanorestore Peggy Gels® and Nanorestore Peggy Gums®, after the PGC.

This paper reports on the evaluation of a PVA TC-PN formulated to be combined with an oil-in-water (o/w) nanostructured fluid (NSF), and specifically targeted to the removal of a polyvinyl acetate (PVAc) non original varnish from the oil painting *The Studio* by Picasso. Despite the diffusion of a large amount of color binders, oil remains one of the most favorite mediums by artists, thanks to its desirable properties and optical qualities. Indeed, oil-based paintings are the most common in the holdings of the PGC. The composition of modern oil paints changed significantly over time. They contain additives such as dryers, fillers, stabilizers, and dispersion agents to stabilize the paint in the tubes whilst controlling the rheology as well as the drying time of the paint [2]. The incorporation of dryers, fillers, dispersion agents, and stabilizers increased during the twentieth century, and over time it has impaired the stability and resistance of the oil paints. The quality of the paint and binder can significantly affect the characteristics of the final paint-film and its subsequent reaction to ageing and treatments [2,3]. Besides, previous conservation treatments may have caused major changes in the chemical or physical characteristics of the paintings, determining their response to ageing and successive treatments. This is the case, for instance, of lining, which can cause the alteration of the paintings surface texture and appearance, as occurred with *The Studio*.

The removal of not original materials from painted surfaces still remains one of the most frequently executed tasks in the conservation of modern and contemporary art, and it requires conservators to make complex decisions. In fact, cleaning is an irreversible and delicate operation, where conservators are required to minimize the risk of interaction between paints and cleaning agents, and the diffusion of solubilized dirt or coatings through the paint layer. This is often problematic, as modern paints additives may increase the sensitivity to cleaning fluids, which could leach and deteriorate the paints. In many cases, the painted layers have a low binder content, which causes pigments to be poorly protected and more solvent-sensitive; moreover, specific colors can show a higher sensibility to water and to solvents employed in conservation treatments. In addition, the roughness of the painted surface, which is typical of modern works of art, makes homogeneous cleaning with traditional tools even more difficult and risky. Indeed, water in cleaning solutions may act both as a reaction medium and as a high polarity solvent, with deep penetration into the micro-porosities of

paint layers, and organic solvents can interact with paint components driving to leaching and swelling phenomena.

In the last decades efforts focused on the development of "gelled-systems" that are capable of retaining liquids and preventing their uncontrolled spreading and vertical diffusion. Cellulose ethers, carboxymethyl cellulose, and polyacrylic acid neutralized with strong bases have been extensively used as thickening agents in order to avoid the use of free cleaning fluids. The intrinsic limit of these thickeners is that they may leave polymer residues on the surface after cleaning, due to the weak interactions between the polymer molecules, and to the poor control of the solvent diffusion. Invasive rinsing steps are thus needed to remove such residues [4–7].

In view of the above issues, one of the main goals in the cleaning of modern and contemporary paintings is the development of novel classes of gels, that are able to minimize the interaction between cleaning fluids and the paint surface thanks to: 1) effective confinement of solvents, i.e. controlled amount of the solvent that is in direct contact with the surface and its limited penetration in the paint layers; 2) absence of residues on the paint surface; 3) selective interaction of the complex fluid with the material to be removed.

Based on such requirements, the study group investigated and tested for the first time a combined system where an o/w NSF, specifically targeted at the removal of the non-original varnish used on *The Studio*, was confined into a TC-PN hydrogel. In the last decades, NSFs have proved to be highly efficient in the swelling and removal of hydrophobic coatings [8–16], as they work through a removal mechanism that, for high molecular weight substances, such as polymers, is based on dewetting and detachment, thus allowing a more controlled surface cleaning with respect to traditional solvent chemistry [17–21]. As mentioned, the use of aqueous fluids on modern oil paints requires special attention, and an optimal strategy is thus to confine cleaning fluids in retentive gel matrices, minimizing the risks to the artifacts [22–30].

The physicochemical characterization of the combined gel-NSF cleaning system includes the interaction of the NSF with the gel and its diffusion inside the gel network, which were investigated using Confocal Laser Scanning Microscopy (CLSM) and Fluorescence Correlation Spectroscopy (FCS). The structure of the combined NSF and gel was analyzed with Small Angle X-ray Scattering (SAXS) in order to check the effects of the confinement on both components.

Preliminary cleaning tests were performed on mock-up samples (made using the original recipes and protocols employed during the 1969 restoration of the work), and monitored through 2D Fourier Transform Infrared Spectroscopy (FTIR) imaging to verify the efficacy of the cleaning as well as the absence of residues; this allowed to define the ideal procedure to be used on the original artwork. The TC-PN gels, loaded with the NSF, were then tested on the painting itself, *The Studio*.

The Case Study

Picasso completed *The Studio* in 1928 in his studio in Paris. The following year he gave it to his dealer, Daniel-Henry Kahnweiler, and five years later he asked the painting to be returned in an unusual exchange for five other paintings, thus demonstrating the importance he attributed to the work. The painting was lent to the Museum of Modern Art in New York for two exhibitions in 1939-40 and in 1941, and then remained in the United States most likely by decision of the artist. Peggy Guggenheim acquired it for her collection in 1942. In the words of Robert Motherwell: "That painting was perhaps the most important influence on my life in those first ten years in New York. That incredible white [. . .], surely one of the most austere and powerful works since the height of Cubism [. . .] unquestionably one of the masterpieces of the 20th century". In 1948, Guggenheim brought the painting to Venice, exhibited it at the Biennale, and then installed it in her home. Since her death in 1979, it has been part of the PGC, the Italian branch of the Solomon R. Guggenheim Foundation, New York.

The painting presents the vivid colors of Synthetic Cubism, but is dominated by a vast expanse of white, with figures defined by geometric, wire-like contours in the manner of Picasso's wire sculptures of the same period. Shortly after completion Picasso returned to the painting and substantially reworked it by overpainting large areas with white and reducing the variety of the palette and the complexity of the composition. The colors underneath the expanse of white paint can be detected with a microscope or even with the naked eye.
Previous conservation logs have been studied in depth to understand materials and methods used by conservators. In 1969, Margaret Watherston examined the painting at the Metropolitan Museum of Art, but she did not identify the earlier version painted by the artist. Her materials, notes, recipes, and photos from her professional career are collected in a series of files [31]. The files that pertain to *The Studio* include the recipes for the wax-resin and the varnish employed in the lining of the work. These materials were confirmed by subsequent studies carried out on the painting. In the condition report Watherston wrote: "Surface of painting is extremely dirty, with numerous pressure and age cracks. Thickness of paint varies considerably, and texture of canvas is exposed in many places. Painting should be given water-chemical treatment on the vacuum table to minimize cracks, then be lined and mounted, if this seems necessary, on a honeycomb panel with linen countermount on the reverse side." At the time, it was thought that to prevent dangerous cracking and flaking one should protect paintings by working on the verso. Therefore, *The Studio* was lined with wax-resin adhesive and mounted on a honeycomb panel, and its recto sprayed with a synthetic final varnish (a PVAc, commercially named AYAC). This ignored the original, unvarnished state of the painting and eliminated visual effects that were previously visible. Over the years the varnish yellowed and affected the areas painted in white. Probably some of the wax migrated trough the outer layer of the paint, partly mixing with the varnish and favoring the embedment of environmental particulate that led to darkening of the surface. In fact, both wax and AYAC (which has a glass transition temperature of 18-33°C depending on its purity) are quite sensitive to temperature fluctuations, and this explains their capacity to embed solid particulate. Over time the delicate tonal contrast of white on white was compromised by the deposits of dust and grime, by the appearance of wax through the cracks, and by the flattening effect of the yellowed varnish that was applied in the late sixties. Therefore, we decided to remove the unauthentic varnish in order to minimize the amount of deposits on the surface and to recover the readability of the paints, especially of the white shades that had been altered by yellowing varnish.

MATERIALS AND METHODS

Chemicals

Polyvinyl alcohol polymers,PVA, (hydrolysis degree = 88%, M_w 100 kDa, and hydrolysis degree 98%, M_w 160kDa) for the hydrogel preparation were purchased from Sigma-Aldrich. $C_{9-11}E_{5,5}$ alcohol ethoxylate (Berol 266®, AkzoNobel), sodium dodecylsulfate (SDS, Sigma-Aldrich, purity ≥ 99%), 2-butanol (BuOH, Sigma- Aldrich, purity 99%), butanone (methyl ethyl ketone, MEK, Sigma-Aldrich, purity 99%) for the NSF preparation, and Bodipy® 558/568 C12 (4,4-difluoro-5-(2-thienyl)-4-bora-3a,4a-diaza-s-indacene-3-dodecanoic acid), ThermoFisher) for CLSM experiments were used as received, without further purification. Water was purified with a Millipore Milli-Q gradient system (resistance > 18 MΩ cm).

NSF Preparation

The selected NSF is composed as follows (w/w): H_2O, 65.9%; $C_{9-11}E_{5,5}$, 3.3%; SDS, 0.2%; BuOH, 9.7%; MEK, 20.9%. The system was prepared by mixing water and the two surfactants at room temperature until a clear solution was obtained. Then the two solvents were included in the formulation and the system was stirred until all the solvent was dissolved either in the continuous aqueous phase or in the micelles. BuOH and MEK are partly water-miscible [32].
A labeled NSF was prepared for Fluorescence Correlation Spectroscopy experiments by adding the amphiphilic dye Bodipy to the formulation (10 nM).

Hydrogel Preparation

PVA "twin-chain" polymer networks (TC-PNs) hydrogels were prepared through a synthetic process, which has been described elsewhere[1]. For the TC-PN used in this study, we selected a 3:1 ratio between the high molecular weight PVA and the low molecular weight PVA, and a single freezing/thawing cycle. Prior to use, gel sheets (e.g. 10 x 20 cm^2) were immersed in the NSF (at least for 24 h) to upload the cleaning fluid.

Painting Mock-up Preparation and Cleaning Procedure

Painting mock-up samples were realized by using Windsor&Newton oil paints (zinc white, cadmium orange, raw Siena, ivory back) brushed on commercially prepared canvas. After 1 year, part of the mock-up samples was relined, using a wax-resin adhesive based on Watherston's original recipe [31]: "5 pounds Beeswax; 5 pounds Multiwax (white synthetic wax); 6 pounds Dammar resin crystals; 2 Pounds of Venice Turpentine." In addition to mock-up samples, several oil paintings and fragments from warehouses and flea markets were used as naturally aged mock-ups in order to provide a further comparison.
All the mock-up samples, either relined or not, were varnished with commercial PVAc (AYAC, Union Carbide, Dow Chemical, USA) dissolved in toluene or methyl alcohol (Sigma-Aldrich), as reported in Watherston's documents. Then, the mock-ups were aged in a light box at 11000 lux for 1 month.
Prior to the application, gel sheets uploaded with the NSF were gently squeezed with blotting paper to remove the excess fluid from their surface. Correct drying of the gel is important for the cleaning process in order to avoid the presence of non-confined solvent on the painting surface.
During application, the contact time of the gel with the paint layer varied from few seconds to 2 minutes. The application caused the varnish and wax layer to swell and soften. Gentle mechanical action with a dry cotton swab allowed the removal of the swollen/softened varnish and wax. Finally, a water-loaded gel was shortly applied on the same spot to remove possible residues of the NSF.

Small-angle X-ray Scattering (SAXS)

Small-angle X-ray Scattering (SAXS) measurements were performed with a HECUS S3-MICRO SWAXS-camera, equipped with a Hecus System 3 2D-point collimator (min divergence 0.4 × 0.9 $mrad^2$) and two position sensitive detectors (PSD-50M), consisting of 1024 channels with a width of 54 μm. During the experiments, the K_α radiation (λ = 1.542 Å) emitted by a Cu anode from the Oxford 50 W microfocus source with customized FOX-3D single-bounce multilayer point focusing optics (Xenocs, Grenoble) was used, while the K_β line was removed by a multilayer filter. The voltage was generated by the GeniX system (Xenocs, Grenoble). The sample-to-detector distance was 26.9 cm. The volume between the sample and the detector was kept under vacuum during the measurements to minimize the scattering from the atmosphere. The camera was calibrated in the small-angle region using silver behenate (d = 58.38 Å). Scattering curves were obtained in the q-range

between 0.01 and 0.6 $Å^{-1}$. The temperature control was set to 25°C. Liquid samples (i.e. the NSFand neat water, used as a reference) were contained in 2 mm thick quartz capillary tubes sealed with hot-melting glue. The gel and NSF-loaded gel samples were contained in a sample holder for solids, with Kapton windows. Desmearing of the SAXS curves was not necessary thanks to the focusing system.

Confocal Laser Scanning Microscopy(CLSM)-Fluorescence Correlation Spectroscopy (FCS)
CLSM-FCS experiments were performed on a Leica TCS SP8 confocal microscope (Leica Microsystems GmbH, Wetzlar, Germany) equipped with a 63X water immersion objective. A fluorescent PVA hydrogel was obtained by labeling high molecular weight PVA with Fluoresceine Isothyocianate (FITC), as previously reported [1], while NSF was labeled with Bodipy, as described above. Imaging of the labeled gel was performed by exciting FITC with the 488 nm laser line (Ar laser) and collecting its fluorescence with a PMT (498-530 nm). The labeled NSF was also observed by imaging, exciting Bodipy with a DPSS solid state laser at 561 nm and collecting its fluorescence at 571-630 nm. FCS experiments were performed by probing the NSF diffusion inside the hydrogel: the fluorescent signal of Bodipy was collected, in this case, by using a hybrid detector (HyD) in the 571-630 nm range.
FCS curves were normalized and averaged (6-10 repetitions per sample). A 10 nM (nanomolar) aqueous solution of Alexa Fluor 568 was used for FCS calibration [33].
The autocorrelation curves were analyzed according to a model that considers the three-dimensional Brownian diffusion of fluorescent species across a 3D-ellipsoidal Gaussian volume as the only phenomenon influencing the decay. The curves were analyzed considering either a one-component decay [34]:

$$G(\tau) = \frac{1}{N}\left[\left(1+\frac{\tau}{\tau_D}\right)^{-1}\left(1+\frac{\tau}{S^2\tau_D}\right)^{-1/2}\right]$$

or a two-components decay [35]:

$$G(\tau) = \frac{1}{N}\left[f_1\left(1+\frac{\tau}{\tau_{D1}}\right)^{-1}\left(1+\frac{\tau}{S^2\tau_{D1}}\right)^{\frac{-1}{2}} + (1-f_1)\left(1+\frac{\tau}{\tau_{D2}}\right)^{-1}\left(1+\frac{\tau}{S^2\tau_{D2}}\right)^{\frac{-1}{2}}\right]$$

where N is the average number of fluorescent molecules detected inside the confocal volume ($N = CV$, with $V = \pi^{3/2}{w_0}^3 S$ and C the concentration), $f_1$is the percentage of the contribution of $\tau_{D,1}$ to the total decay time, $\tau_{D,i}$ are the decay times, and $S = z_0/w_0$ is the ratio between the axial and the lateral dimensions of the confocal volume, determined through the calibration procedure with Alexa 568. The diffusion coefficients D_i of the labeled species can be determined by:

$$\tau_{D,i} = \frac{{w_0}^2}{4D_i}$$

2D-Imaging Fourier-transform Infrared Spectroscopy (FTIR)
The 2D imaging-FTIR analysis on painting mock-ups was carried out using a Cary 620-670 FTIR microscope, equipped with an FPA 128x128 detector (Agilent Technologies). This set up allows the highest spatial resolution currently available to FTIR microscopes. The spectra were recorded directly on the surface of the samples (or of the Au background) in reflectance mode, with open aper-

ture and a spectral resolution of 8 cm^{-1}, acquiring 128 scans for each spectrum. A "single-tile" analysis results in a map of 700 x 700 μm^2 (128 x 128 pixels), and the spatial resolution of each imaging map is 5.5 µm (i.e. each pixel has dimensions of 5.5 x 5.5 μm^2). Multiple tiles can be combined in mosaics. In each 2D map, the intensity of characteristic bands of the varnish, or of the gel, was imaged. The chromatic scale of the maps shows increasing absorbance of the bands as follows: blue < green < yellow < red.

RESULTS AND DISCUSSION

The constant dialogue between conservators and scientists allowed to define the main requirements that novel materials and systems must fulfill to overcome the limitations of traditional cleaning methods. Besides the ability to effectively remove the aged PVAc varnish from the painting's surface, such requirements include: 1) Reduction of the toxicity of cleaning materials to decrease risks to operators and the environment; this was tackled by adopting non-toxic gel components and an aqueous nanostructured fluid (NSF) with reduced amount of organic solvents; 2) The use of a thermodynamically stable cleaning fluid with low surfactant content, which was addressed by selecting the NSF used in this study; 3) Complete avoidance of free, non-confined cleaning fluids (including rinsing steps), which was addressed by confining the NSF in the hydrogel; 4) The use of highly retentive gels, to control the amount of fluid in direct contact with the varnish and to maintain the fluid at the varnish-paint interface without excessive penetration; this grants control of the cleaning action in response to subtle differences in paint sensitivity and varnish/soiling behavior, and maximizes the cleaning efficacy, reducing the need of mechanical action; 5) Optimal mechanical properties of the gels, i.e. high viscoelasticity and flexibility, which grant the capacity to adapt to complex and clotted paint surfaces, the easy handling of the gels, and the absence of gel residues left on the surface after cleaning.

The TC-PNs hydrogels were synthesized and optimized to meet these requirements, and an extensive characterization of the type of structure, rheological properties, and PVA dynamics in the gel network, has been recently provided for the formulation used on the paintings by Pollock, *Two* and *Eyes in the Heat* [1]. The TC-PN used in this study has similar characteristics, but a slightly different formulation and some structural differences (detailed in the following paragraphs) owing to the presence of the o/w nanostructured fluid.

The TC-PNs gels are opalescent and offer optimal mechanical properties and solvent retention. They are flexible and elastic, and their controlled release of uploaded fluids grants the possibility of varying the fluids contact time with the paint surface, controlling the interaction between solvents and paint layers. These features have already established the TC-PNs as suitable tools for the cleaning of modern and contemporary art in previous case studies [1,36,37], which proved that their synthetic process can be feasibly tuned and changed in order to vary the gels' characteristics and to adapt them to specific needs.

The loading of the gel with the NSF was obtained simply by immersing a piece of gel in an excess of NSF for at least 24 hours, according to our previous experiments with these systems. Previous studies demonstrated that similar gels exhibit a structure and porosity that allows aqueous NSFs to be loaded in the gel without disrupting the structure of the gel and the fluid, thus demonstrating that the cleaning properties of the combined system are not altered [25,29]. However, in view of the application of the system in the cleaning of a Picasso masterpiece, SAXS and FCS measurements were carried out also in this case, in order to study the interaction of the gel with the NSF. SAXS analyses were performed on the sole hydrogel and NSF, and on the combined NSF-loaded hydrogel. Figure 1 shows the resulting scattering profiles together with their best fitting curves, while Tables

1 and 2 report the main fitting parameters obtained by the analysis of the curves. A cleaning system similar to the NSF here reported was recently investigated by means of SANS analyses [20], and was found to be constituted of elongated ellipsoidal micelles dispersed in a water/BuOH/MEK continuous phase. The shape and size of supramolecular aggregates was attributed to the proximity of the system to the nonionic surfactant's cloud point at room temperature. In this study, a close NSF formulation was used, but with a substantial variation, i.e. a small amount of SDS (0.2 % w/w) was included in the system, in order to optimize the cleaning capacity by increasing the surfactant cloud point. Moreover, having a cloud point significantly higher than room temperature can be crucial in practical applications, and the addition of even very low concentrations of ionic surfactants to nonionic surfactants-based systems is well known to drastically increase the clouding temperature [37–40]. This is due to the increase of surface charge of the disperse phase droplets, which confers a slight repulsion between the aggregates [38,39]. The overall effect is the stabilization of the system even at temperatures at which the nonionic surfactant alone would have phase-separated. For this main reason, the nonionic/ionic mixed micelles, in this case, could be fitted only using a spherical model, differently from the cited paper, where the aggregates were elongated.
More in detail, after several attempts using a range of possible different models, the best fitting was obtained by considering the NSF micelles as non-interacting polydisperse core-shell spheres, defined by two contrasts, i.e. bulk/shell and shell/core. The scattering length density (SLD) of bulk, shell and core, i.e. ρ_{bulk}, ρ_{shell} and ρ_{core} respectively were calculated according to the SLD of each chemical included in the formulations. For globular micelles of homogeneous scattering length density, the total scattered intensity $I(q)$ (cm^{-1}) is given by [42,43]:

$$I(q) = N_P V_P^2 \Delta\rho^2 P(q) S(q) + \text{bkg}_{\text{inc}}$$

where N_p is the number density of the scattering particles (cm^{-3}), V_p is the volume (cm^3), $\Delta\rho$ is the contrast term (cm^{-2}), $P(q)$ is the form factor and $S(q)$ is the structure factor. In this case $S(q) = 1$, as the particles were considered to be non-interacting due to the very low concentration of the anionic surfactant. In the case of spherical core-shell aggregates, the particle scattering intensity is expressed as follows [44]:

$$I(q) = \frac{\phi}{V_P}\left[(\rho_{core} - \rho_{shell})\frac{3V_c j(qr_c)}{qr_c} + (\rho_{shell} - \rho_{bulk})\frac{3V_P j(qr_s)}{qr_s}\right]^2$$

where $j(x)$ is expressed as:

$$j(x) = \frac{(sinx - xcosx)}{x^2}$$

and where ϕ is the volume fraction of the micellar phase, V_c is the core volume, r_c is the core radius, $r_s = r_c + t$ (t is the shell thickness). Since this model takes into account a polydisperse core, which follows the Schultz distribution, the form factor is normalized by the average particle volume:

$$\langle V \rangle = \frac{4\pi}{3}\langle r_c^3 \rangle$$

where:

$$\langle r_c^3 \rangle = \frac{(z+2)(z+3)}{(z+1)^2} \langle r_c \rangle$$

and z is the width parameter of the Schultz distribution [45]:

$$z = \frac{1}{\left(\frac{\sigma}{\langle r_c \rangle}\right)^2} - 1$$

being σ^2 the variance of the distribution. The polydispersity index (PDI), reported in Table 1 is defined as $\sigma/\acute{a}r_c\tilde{n}$ and its value is comprised between 0 and 1.

Table 1. SAXS fitting parameters obtained by the analysis of the NSF scattering profile.

Fitting parameter	Best value
Core radius, r (Å)	10.1 ± 0.1
Shell thickness, t (Å)	15.2 ± 0.1
Core polydispersity index (PDI)	0.58 ± 0.01
SLD_{core} (10^{-6} Å^{-2})	7.8
SLD_{shell} (10^{-6} Å^{-2})	9.5
SLD_{bulk} (10^{-6} Å^{-2})	8.8

Figure 1 reports the best fitting obtained using the core-shell model. An average core radius, r, of 10 Å was obtained by the fitting, which is reasonably in agreement with the 14 Å theoretical length for an average 10 carbon atoms aliphatic chain, as calculated using the Tanford's formula [46]. The core polydispersity is quite high, but this value likely reflects the fact that the nonionic surfactant itself actually is a mixture of different chemical species having a distribution both for the aliphatic chain length (9-11 carbon atoms) and for the polyethoxylate polar head chain (5.5 CH_2CH_2O- units, in average).

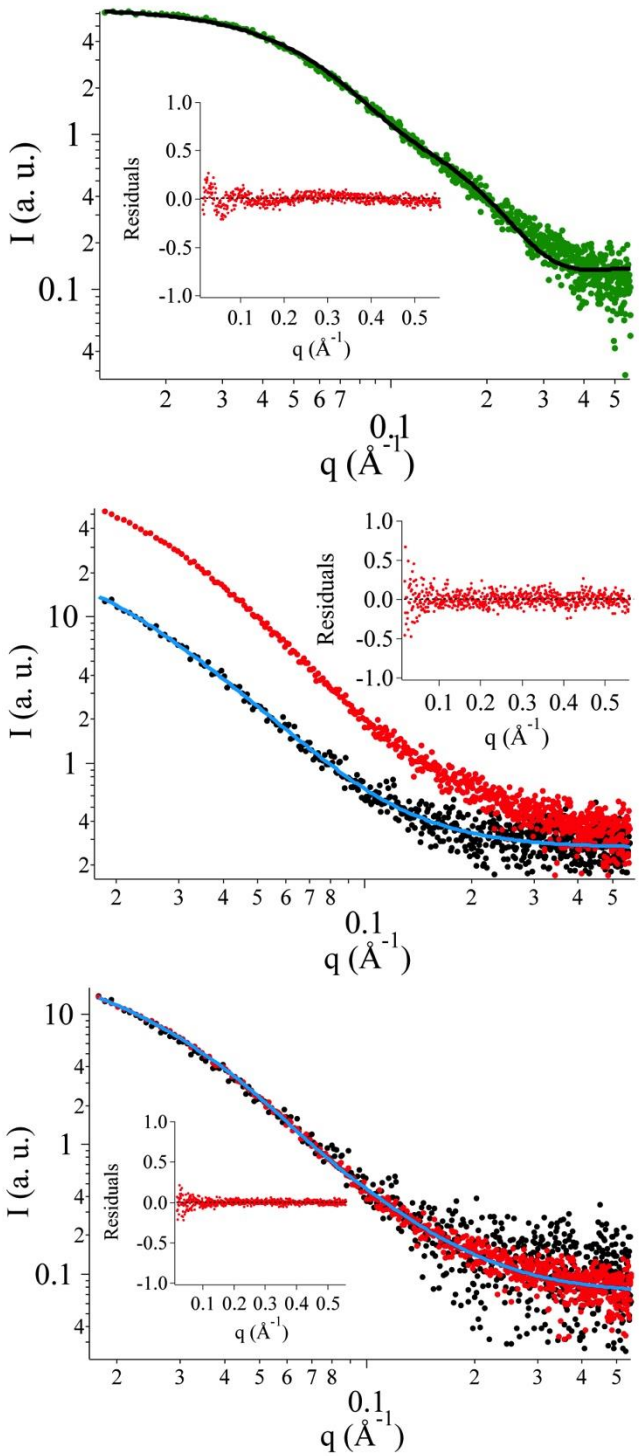

Figure 1. SAXS scattering curves. *Top graph*: neat NSF (green circles), together with its best fitting curve (solid black line), and residuals' fitting (inset). *Middle graph*: neat TC-PN (black circles), together with its best fitting (solid blue line), and residuals' fitting (inset); NSF-loaded TC-PN (red circles). *Bottom graph*: NSF-loaded TC-PN after the mathematical treatment described in the text (red circles), superimposed to the scattering curve of the neat hydrogel (black circles), together with its best fitting (solid blue line), and residuals' fitting (inset). The three residuals' plots show that the fitting is good, since no significant peaks, trends, or other features are visible in the graphs, and the points are uniformly distributed below and above zero, along the *q*-axis.

Moreover, a system composed by mixed micelles of nonionic/ionic surfactants in the presence of two water-miscible solvents, which are partitioned between the aqueous and the micellar phase, is

structurally more complex than classically-defined o/w microemulsions composed of water/oil/surfactant and whose PDI usually does not exceed 0.2-0.4 [47,48]. The shell thickness is quite high, as usually is for systems based on alcohol ethoxylates with medium/long polar head chains, but in agreement with the data obtained on previous systems based on the same or similar surfactants [18,19,49,50]. Finally, the SLD of the continuous phase is consistent with the almost complete solubilization of both BuOH and MEK in the ethoxylates groups/water, with little penetration of organic solvents in the micelles' hydrophobic core.
The fitting model for the neat TC-PN was chosen, according to published papers on similar systems [1,51,52], as the sum of two superimposed contributions to the scattered intensity, due to fixed polymer junctions (i.e. the solid-like tie points of the network) and to the polymer chains the gel water-rich environment, respectively. The scattered intensity, *I(q)*, is then modeled as follows:

$$I(q) = I_L(0)\frac{1}{\left[1+\frac{D+1}{3}(q^2\xi^2)\right]^{\frac{D}{2}}} + I_G(0)exp(-q^2R^2/3) + B$$

where $I_L(0)$ and $I_G(0)$ are the Lorentzian and the Guinier parameters, D is the fractal exponent, ξ is a correlation length, R is the radius of gyration of solid-like scattering objects, and B is an incoherent background scattering. Table 2 reports the fitting parameters obtained by the analysis of the experimental scattering curves.

Table 2. SAXS fitting parameters obtained by the analysis of the hydrogel and the NSF-loaded TC-PN scattering profiles.

Fitting parameter	TC-PN	NSF-loaded TC-PN
$I_L(0)$ (cm^{-1})	31 ± 2	25 ± 4
$I_G(0)$ (cm^{-1})	0.3 ± 0.1	2.7 ± 1.0
D	2.5 ± 0.1	2.5 ± 0.2
ξ (nm)	5.1 ± 0.5	5.1 ± 1.0
R (nm)	3.2 ± 0.8	4.9 ± 0.4

Considering previous studies on PVA-based hydrogels [53], R was assumed to be the radius of gyration of PVA crystallites in the solid-like portions of the gel, while ξ can be seen as a characteristic length of the polymeric network in the water-rich gel regions, where polymer chains are less constrained. This dimension depends on the local concentration of polymer, and it is strongly dependent on synthetic pathway.
The fitting values obtained for the neat hydrogels are in perfect agreement with the ones obtained in a previous study, which included the same formulation used here, among other PVA-based gels [1]. In particular, the fractal exponent, D, of 2.5 (PVA gels usually show fractal exponents in the 2 – 4 range), a correlation length, ξ, of about 5 nm, and PVA crystallites of about 3 nm (R) are also in

agreement with previous observations on PVA hydrogels [54]. Finally, the quite high value of the $I_L(0)/I_G(0)$ ratio indicates that the number of solid-like scattering objects (crystallites) is limited. [1].
The analysis of the scattering curve of the NSF-loaded TC-PN was not straightforward. Figure 1 (middle graph) shows that the scattering profiles of the NSF-loaded TC-PN (red circles) and of the neat hydrogel (black circles) look similar, apart from a multiplicative factor. Actually, the NSF-loaded TC-PN curve also includes scattering signals coming from the NSF, which are not easily isolable from the curve, because the NSF scattering curve does not present particular features, such as peaks or bumps. The adopted fitting strategy based on the assumption that the NSF structure inside the gel was not significantly altered, as actually found in a previous study on the loading of NSFs into different hydrogels [25]. Therefore, it should have been possible to separate the contributions of both the NSF and the sole hydrogel to the total scattering intensity. The experimental scattering curves of these two samples (i.e., the NSF and the TC-PN) were linearly combined, and it was found that:

$$0.2 \times \text{“NSF”} + 4 \times \text{“TC-PN”} = \text{“NSF-loaded TC-PN”}$$

In other words, when the opportunely scaled NSF scattering curve was subtracted from the NSF-loaded TC-PN curve, the resulting curve, divided by a factor 4 (red circles), could be superimposed almost perfectly to the sole hydrogel curve (black circles), as shown in Figure 1 (bottom graph). This curve was fitted using the model described above and, as predictable, the fitting parameters obtained did not significantly differ from the ones of the neat TC-PN (compare second and third column in Table 2). The factor 4 between the TC-PN curve and the “subtracted curve” is actually easily explainable in view of the different SLD of the solvent in the gel, when water was replaced by the continuous phase of the NSF, where significant amounts of BuOH and MEK were dissolved. Looking at the other parameters, a slight increase in the size of the solid-like domains in the gel (4.9 nm vs. the initial 3.2 nm size) and a decrease of the $I_L(0)/I_G(0)$ ratio are observed, which can be ascribed possibly to the interaction of the polymer network with organic solvents and surfactants included in the NSF. The slight increase of R might be due to the lower affinity of PVA towards water/BuOH/MEK with respect to water alone. In the peripheral regions of crystallites, PVA chains are normally more hydrated and less tightly packed than in the crystallites core; in the presence of a worse solvent than water, the looser chains start to interact more tightly and collapse, leading overall to an increase of the crystallites core. Since the structure becomes more crowded, this could also explain the decrease of the $I_L(0)/I_G(0)$ ratio. Apart from these changes, both the NSF and the TC-PN have shown to preserve their nanostructure and, subsequently, their cleaning properties are expected to be maintained in view of a potential application.
According to the literature [55], PVA, even when highly hydrolyzed, interacts with both anionic and nonionic surfactants through hydrophobic interactions between the polymer carbon-chain skeleton and the hydrophobic tails of the surfactants. Therefore, the hydrophilicity of the polymer increases, especially in the case of polymer-anionic surfactant interactions: in this case, the network becomes a polyelectrolyte hydrogel [56].
CLSM imaging of the labeled gel and NSF confirms that an interaction occurs when the NSF is loaded in the gel (see Figure 2A, B): the pattern of the gel porosity (green, Figure 2A) is closely traced by the fluorescent signal of labeled micelles (red, Figure 2B), suggesting that micelles are able to stick on the gel walls. Overall, the macroporosity of the gel was not significantly altered by loading with the NSF.
The diffusion of the NSF in the TC-PN’s pores was investigated through FCS and compared to the diffusion of the free NSF. The free NSF decay curve can be described by a single diffusion coefficient (see Table 3 and Figure 2C). The hydrodynamic diameter of the micelles ($d_H \cong 5.0 \pm 0.4$ nm)

evaluated through the Stokes-Einstein equation, using the diffusion coefficient obtained by FCS fitting and assuming the viscosity of the NSF to be the same as water at 25˚C, is in agreement with the micelle dimension obtained through the fitting of SAXS (ca. 5 nm, see Table 1). The diffusion of the NSF inside the gel, FCS curves could be described only considering a two-component decay. In fact, the diffusion coefficient characterizing the free NSF can still be detected inside the gel pores after loading, and accounts for the 60% ca. of the total decay. However, a slower component was detected as well, probably due to the micelle-gel interaction (see Table 3). CLSM and FCS prove that micelles are able to diffuse through the gel matrix, but also interact with the gel walls. Overall, the combination of the SAXS and CLSM/FCS results suggests that such interaction probably takes place in the more external and less crowded regions of the gel walls, rather than in the crystallites.
When the system is in contact with a substrate, the cleaning process is granted by the osmotic equilibrium inside the network: while the NSF freely diffusing in the outer pores interacts with the painted surface and modifies, fresh NSF is recalled, due to the interconnected porosity and the free/bound micelles equilibrium.
In other words, the micelles diffusion dynamics are altered after the NSF confinement in TC-PNs. At the same time, the uncontrolled spreading of the cleaning fluid is avoided. Therefore, a time- and space-controlled cleaning action results, not achievable when non-confined fluids are used.

Table 3. NSF diffusion coefficients (D, $\mu m^2/s$) and their contribution to the total FCS decay (f, %), before (free NSF) and after (NSF in the TC-PN) loading inside the hydrogel.

	Free NSF	**NSF in the TC-PN**
D_1 ($\mu m^2/s$)	100 ± 6	100
f_1(%)	100	60 ± 16
D_2 ($\mu m^2/s$)	--	7 ± 4

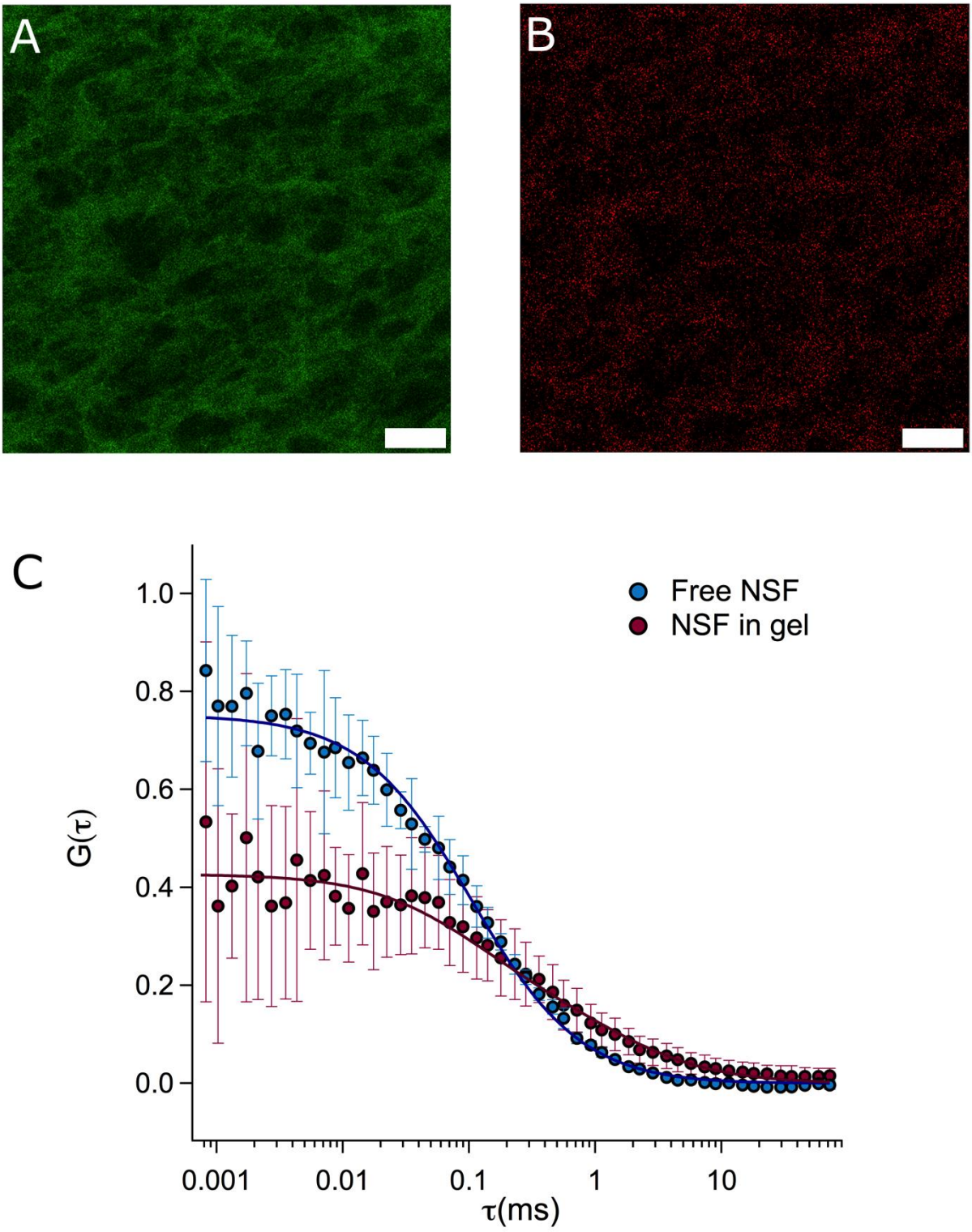

Figure 2. CLSM images of the TC-PN after the loading with NSF: (A) the fluorescence of FITC-labeled PVA (green) shows the gel structure; (B) the fluorescence of Bodipy-labeled NSF (red) seems to trace the gel porosity, suggesting that some micelles are interacting with the gel walls. Scale bar is 20 μm long. (C) FCS autocorrelation curves describing the diffusion of the NSF before (blue markers) and after (purple markers) loading inside the TC-PN.

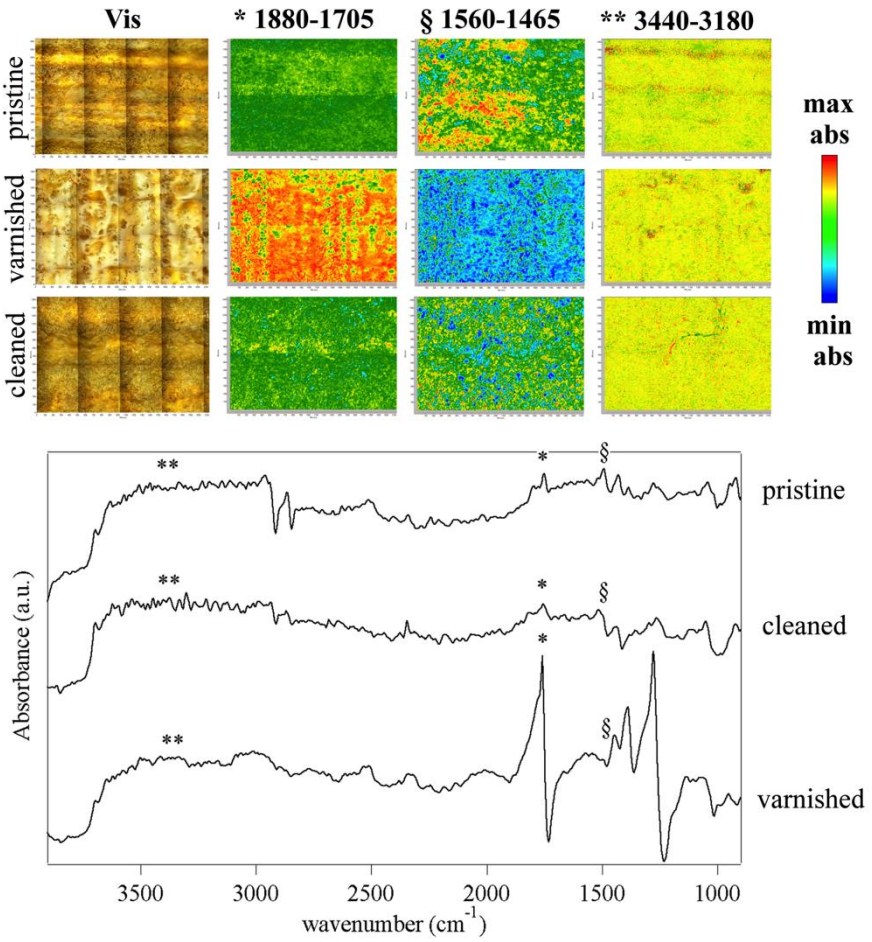

Figure 3. FTIR 2D imaging of paintings' mock-up samples. Top panel: visible light and 2D FTIR maps of mock-ups that were unvarnished (top row), varnished (center row), or varnished and then cleaned with the PVA hydrogels loaded with the o/w nanostructured fluid (bottom row). For each sample, the images beside the visible map show the corresponding 2D FTIR maps, where the intensities of the peaks in the 1880-1705 cm^{-1} (C=O stretching, polyvinyl acetate-based varnish), 1560-1465 cm^{-1} (CH_2 bending, wax used in the lining), and 3440-3180 cm^{-1} (where characteristic the OH stretching band of PVA would be found in case of gel residues after cleaning) were imaged. All maps have dimensions of 2100 x 1400 μm^2, each axis tick being 50 µm. The FTIR Reflectance spectra are shown in the bottom right panel, each spectrum relating to a single pixel (5.5 x 5.5 μm^2) of the corresponding 2D imaging map. The maps show the removal of the varnish and surface removal of wax spots, while no absorptions ascribable to PVA could be detected.

Cleaning tests on mock-up samples showed that it was possible to remove the wax lining residues along with the PVAc varnish. Reduced application times (5-10 s) produced lesser softening of the PVAc layer, keeping the cleaning action more superficial. The softening of the varnish increases with longer contact times. After ca. 40-60 seconds PVAc became streaky, but still well separated from the paint layer. The short contact times and controlled fluid release from the gel allowed avoiding uncontrolled penetration of varnish and damages to the paint layer. Rinsing steps with gels simply loaded with water (applied to the painting surface for 1-2 second) made the usage of free liquids on the surface unnecessary. Mock-up samples, lined or not, showed similar positive response to the cleaning methodology. After the cleaning tests, observation under microscope and UV lamp showed the cleaning efficacy of the method. A more detailed assessment was obtained through FTIR 2D imaging. Figure 3 shows the visible light microscope images and FTIR 2D imaging of mock-ups that mimic the lined painting by Picasso. The application of the NSF-loaded hydrogel on the surface of the mock-ups led to the removal of the PVAc-based varnish, as observed under visible light and by the disappearance of the characteristic bands of PVAc (e.g. C=O stretch-

ing in the 1880-1705 cm^{-1} region) from the spectra recorded on the samples' surface. The application of the gel also allowed the surface removal of wax spots (due to the relining intervention), as shown by the decrease of the characteristic band of wax around 1475 cm^{-1} (CH_2 bending); in the varnished mock-up, the band is not observable, as the wax spots are likely covered by the poly(vinyl acetate) layer. The 3440-3180 cm^{-1} region of the spectra was also imaged, where the most intense absorption of PVA (OH stretching) should be observed in case of detectable gel residues left on the surface after the cleaning intervention. No difference in the absorbance intensity was observed in the spectra of the samples treated with the gels with respect to pristine samples; therefore, it was concluded that no detectable gel residues were left by the treatment. The absence of gel residues was expected, considering that the PVA TC-PN hydrogels exhibit a mechanical behavior typical of chemical gels, despite being physical networks (i.e. held by secondary bonds) [1].
No relevant bands ascribable to the surfactants used in the NSF were observed. Alcohol ethoxylate surfactants, such as $C_{9-11}E_{5,5}$, have a characteristic FTIR band around 1120 cm^{-1} (C-O stretching), while SDS has a characteristic peak centered at 1220 cm^{-1} (asymmetric stretching of OSO_3); no significant bands at those wavelengths were observed in the spectra of the cleaned painting mock-up, as compared to pristine samples. Besides, the application of a water-loaded gel after cleaning leads to the absorption of possible surfactant residues, making the cleaning "free" of any possible residue on the painting.
It must be noticed that the detection limit of an FPA detector has been reported to be significantly lower than that of conventional mercury cadmium telluride (MCT) detectors, when trace amounts of materials are considered; in fact, in that case the heterogeneous distribution of the analyte can result in small areas with high localized concentration, which can be detected thanks to the spatial resolution of the FPA detector [57]. In a previous work, a detection limit of ca. 0.02 $pg/\mu m^2$ for the detection of PVA was found, using the same FPA detector and instrumental setup [1]. Overall, we concluded that the cleaning procedure led to the removal of the varnish and wax contaminants, without leaving detectable residues of the gel or of the NSF.
Following the tests on the mock-up samples, the NSF-loaded hydrogels were used for the cleaning of Picasso's *The Studio*. The tests (see Figure 4) confirmed that the PVAc-based varnish was swollen after ca. five seconds of contact with the gel, and then the swollen varnish was gently and easily peeled off with a dry cotton swab just like a second skin, with no alteration of the color layers. Figures 5 and 6 show the painting before, during, and after the cleaning intervention.

Figure 4. The cleaning of Pablo Picasso, *The Studio*, 1928, oil and black crayon on canvas, 161.6 x 129.9 cm, Peggy Guggenheim Collection, Venice (The Solomon R. Guggenheim Foundation, New York). (A) The TC-PN hydrogel is uploaded with the o/w NSF (24h immersion). (B) Gel sheets uploaded with the NSF are gently squeezed with blotting paper to remove the fluid excess from their surface, and (C) cut to desired shape and size. (D) The gel is applied onto the painted surface. (E) Gentle mechanical action with a dry cotton swab allows the removal of the swollen/softened varnish and wax. (F) Rinsing step, a water-loaded gel is shortly applied on the same spot to remove possible residues of the NSF. At bottom, center panel and related black boxed details show the cleaning of white and red areas. On the right, the painting during the cleaning: the cleaned lighter areas can be easily distinguished from the darker uncleaned areas at the top.

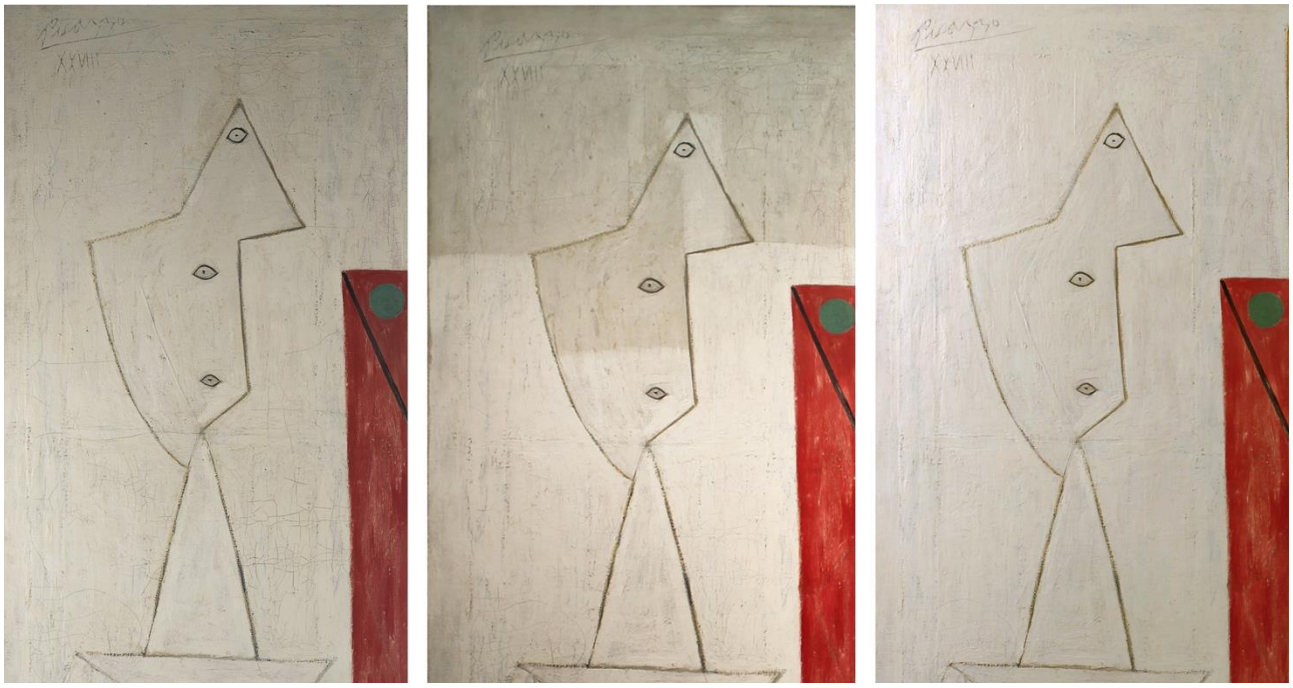

Figure 5. Pablo Picasso, *The Studio*, 1928, Peggy Guggenheim Collection, Venice (The Solomon R. Guggenheim Foundation, New York), before (left), during (center), and after (right) the cleaning carried out with TC-PN hydrogels loaded with the o/w NSF.

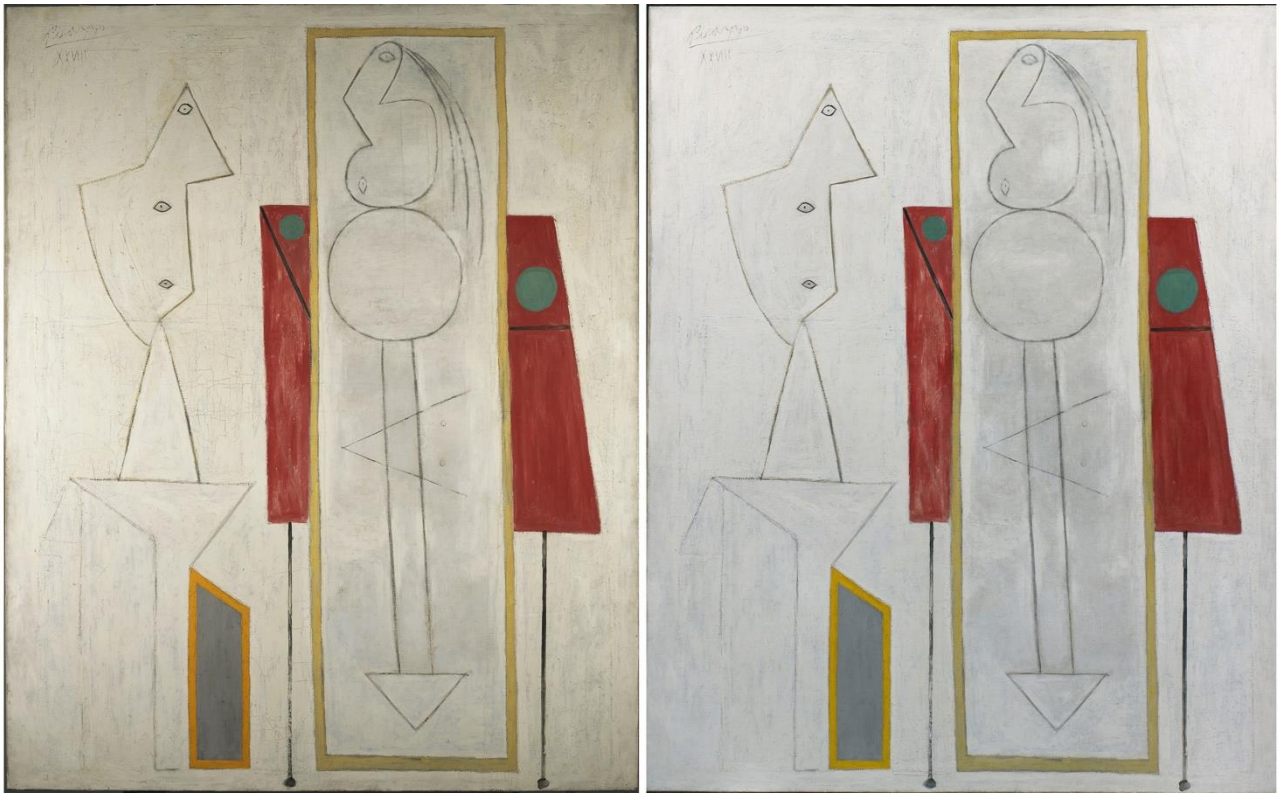

Figure 6. Pablo Picasso, *The Studio*, 1928, Peggy Guggenheim Collection, Venice (The Solomon R. Guggenheim Foundation, New York), before (left) and after (right) the cleaning carried out with TC-PN hydrogels loaded with the o/w NSF.

CONCLUSIONS

Polyvinyl alcohol (PVA) "twin-chain" polymer networks (TC-PNs) hydrogels were combined with a nanostructured fluid (NSF), and the resulting complex system was used to remove non-invasively the aged varnish and wax layer from the surface of Pablo Picasso, *The Studio* (1928). The NSF loading within the TC-PNs was associated to interactions between the NSF and the TC-PN that takes place in the more external and less crowded regions of the gel walls, rather than in the internal crystallites, without significant alteration of the system's components. The diffusion of the complex fluid in the gel matrix and at the gel-painting interface, during cleaning, is granted by the osmotic balance in the network. Overall, these factors guarantee the effective and controlled cleaning action of the gel+NSF system.

Cleaning tests on painting mock-ups showed that the NSF-loaded TC-PNs allow the swelling and softening of varnish and wax layers, which can then be removed with gentle mechanical action using dry cotton swabs, with no mechanical stress to the painted layers. FTIR 2D imaging confirmed the removal of varnish and wax at the micron scale, with no observable residues of the gel or of the NSF (down to the detection limit of the FPA detector, ca. 0.02 pg/μm^2). The removal of the aged PVAc varnish and wax layer from the surface of the painting was then carried out by using the same cleaning protocol successfully tested on the mock-ups. The use of the combined gel+NSF system

allowed a highly effective and safe cleaning action thanks to the controlled wetting and swelling of the painting surface, and the easy mechanical removal of the swollen PVAc layer, without affecting the color layer. It is worth mentioning that TC-PNs gels with the confined NSFs allow the restorer/conservator to choose the most appropriate NSFs contact time with the painting surface for the cleaning operation. In the present case the chosen contact time was of about 5 seconds, which was enough to obtain a perfect swelling of the layer to be removed, without interacting with the original pictorial layer. These results set NSF-loaded PVA TC-PNs as a robust and reliable tool for the cleaning of sensitive paintings, opening new perspectives in the conservation of works of art.

ACKNOWLEDGMENTS

The Italian Consorzio Interuniversitario per lo Sviluppo dei Sistemi a Grande Interfase, CSGI (Center for Colloid and Surface Science), MUR PRIN- 2017249YEF, and the European Union Horizon 2020 projects NANORESTART (Nanomaterials for the Restoration of Works of Art) and APACHE (Active & Intelligent Packaging Materials and Display Cases as a Tool for Preventive Conservation of Cultural Heritage), under the Horizon 2020 Research and Innovation Programme Grant Agreements 646063 and 814496, respectively, are gratefully acknowledged for the financial support. The authors also acknowledge Chiara Barbieri, Director of Publications and Special Projects, Peggy Guggenheim Collection.

DECLARATION SECTION

List of abbreviations

All acronyms and abbreviations are written in full letter when they first appear

Ethics approval and consent to participate

Not applicable

Availability of data and materials

All the available data have been included in the article.

Competing interests

The authors declare no conflict of interest.

Funding

This research has received funding from the European Union NANORESTART (Nanomaterials for the Restoration of Works of Art), APACHE (Active & Intelligent Packaging Materials and Display Cases as a Tool for Preventive Conservation of Cultural Heritage), under the Horizon 2020 Research and Innovation Programme Grant Agreements 646063 and 814496 respectively, and CSGI (Center for Colloid and Surface Science, Progetti Competitivi), MUR PRIN- 2017249YEF.

Authors' contributions

LPB and MLP (PGC) researched the appearance and the art historical context of the painting, and defined the specific and broader aims of the cleaning treatment. MLP and LPB documented the evaluation of cleaning materials, managed the acquired data for the evaluation phase and treatment, and the technical and conservation images and documentation. MLP prepared the mock-up samples and performed the cleaning tests on all mock-ups. LPB performed the cleaning tests on the painting, and carried out the full conservation treatment and the technical examination of the painting.
PB (CSGI) conceptualized the PVA TC-PN gel series and their application to Cultural Heritage conservation; MB, RM and DC carried out the physico-chemical characterization of the gel and NSF, and the 2D FTIR assessment of the cleaning treatment on mock-ups. PB, MB, RM, DC and RG analyzed the data.
All authors contributed to the present text.

Authors' Information

LPB (PGC) designed, led and managed the Peggy Guggenheim Collection contribution to the NANORESTART project, and was the PGC NANORESTART conservator for this case study (2017–2018). MLP was the PGC NANORESTART conservation researcher (2017–2019).
The NANORESTART project was led by PB (CSGI); DC and RG (CSGI) were project coordinator contacts. MB (CSGI) was a post-doctoral researcher during the project, and RM a PhD student at CSGI and the Department of Chemistry, University of Florence.

[@] Piero Baglioni and Michele Baglioni are not related.

REFERENCES

1. Mastrangelo R, Chelazzi D, Poggi G, Fratini E, Pensabene Buemi L, Petruzzellis ML, et al. Twin-chain polymer hydrogels based on poly(vinyl alcohol) as new advanced tool for the cleaning of modern and contemporary art. Proc Natl Acad Sci U S A. 2020;117:7011–20.

2. Learner T. Modern paints: uncovering the choices. In: Learner T, Smithen P, Krueger J, Schilling MR, editors. Mod Paints Uncovered Proc Mod Paints Uncovered Symp. Los Angeles: Getty Conservation Institute; 2007.

3. Burnstock A, van den Berg KJ. Twentieth Century Oil Paint. The Interface Between Science and Conservation and the Challenges for Modern Oil Paint Research. In: van den Berg KJ, Burnstock A, de Keijzer M, Krueger J, Learner T, Tagle de Alberto, et al., editors. Issues Contemp Oil Paint [Internet]. Cham: Springer International Publishing; 2014 [cited 2020 Apr 15]. p. 1–19. Available from: https://doi.org/10.1007/978-3-319-10100-2_1

4. Domingues JAL, Bonelli N, Giorgi R, Fratini E, Gorel F, Baglioni P. Innovative Hydrogels Based on Semi-Interpenetrating p(HEMA)/PVP Networks for the Cleaning of Water-Sensitive Cultural Heritage Artifacts. Langmuir. 2013;29:2746–55.

5. Casoli A, Cremonesi P, Isca C, Groppetti R, Pini S, Senin N. Evaluation of the effect of cleaning on the morphological properties of ancient paper surface. Cellulose. 2013;20:2027–43.

6. Volk A, Berg KJ van den. Agar – A New Tool for the Surface Cleaning of Water Sensitive Oil Paint? In: Berg KJ van den, Burnstock A, Keijzer M de, Krueger J, Learner T, de AT, et al., editors. Issues Contemp Oil Paint [Internet]. Springer International Publishing; 2014 [cited 2016 Sep 27]. p. 389–406. Available from: http://link.springer.com/chapter/10.1007/978-3-319-10100-2_26

7. Burnstock A, White R. A preliminary assessment of the agingidegradation of Ethomeen c-12 residues from solvent gel formulations and their potential for inducing changes in resinous paint media. Stud Conserv. 2000;45:34–8.

8. Giorgi R, Baglioni M, Berti D, Baglioni P. New Methodologies for the Conservation of Cultural Heritage: Micellar Solutions, Microemulsions, and Hydroxide Nanoparticles. Acc Chem Res. 2010;43:695–704.

9. Baglioni M, Rengstl D, Berti D, Bonini M, Giorgi R, Baglioni P. Removal of acrylic coatings from works of art by means of nanofluids: understanding the mechanism at the nanoscale. Nanoscale. 2010;2:1723.

10. Baglioni M, Giorgi R, Berti D, Baglioni P. Smart cleaning of cultural heritage: a new challenge for soft nanoscience. Nanoscale. 2012;4:42.

11. Baglioni M, Berti D, Teixeira J, Giorgi R, Baglioni P. Nanostructured Surfactant-Based Systems for the Removal of Polymers from Wall Paintings: A Small-Angle Neutron Scattering Study. Langmuir. 2012;28:15193–202.

12. Baglioni M, Jàidar Benavides Y, Berti D, Giorgi R, Keiderling U, Baglioni P. An amine-oxide surfactant-based microemulsion for the cleaning of works of art. J Colloid Interface Sci. 2015;440:204–10.

13. Baglioni M, Jáidar Benavides Y, Desprat-Drapela A, Giorgi R. Amphiphile-based nanofludis for the removal of styrene/acrylate coatings: Cleaning of stucco decoration in the Uaxactun archeological site (Guatemala). J Cult Herit. 2015;16:862–8.

14. Baglioni M, Poggi G, Jaidar Benavides Y, Martínez Camacho F, Giorgi R, Baglioni P. Nanostructured fluids for the removal of graffiti – A survey on 17 commercial spray-can paints. J Cult Herit [Internet]. [cited 2018 Jun 19]; Available from: https://www.sciencedirect.com/science/article/pii/S1296207418301110

15. Chelazzi D, Giorgi R, Baglioni P. Microemulsions, Micelles, and Functional Gels: How Colloids and Soft Matter Preserve Works of Art. Angew Chem Int Ed Engl. 2018;57:7296–303.

16. Chelazzi D, Bordes R, Giorgi R, Holmberg K, Baglioni P. The use of surfactants in the cleaning of works of art. Curr Opin Colloid Interface Sci [Internet]. 2020 [cited 2020 Feb 4]; Available from: http://www.sciencedirect.com/science/article/pii/S1359029419301037

17. Raudino M, Selvolini G, Montis C, Baglioni M, Bonini M, Berti D, et al. Polymer Films Removed from Solid Surfaces by Nanostructured Fluids: Microscopic Mechanism and Implications for the Conservation of Cultural Heritage. ACS Appl Mater Interfaces. 2015;7:6244–53.

18. Baglioni M, Montis C, Brandi F, Guaragnone T, Meazzini I, Baglioni P, et al. Dewetting acrylic polymer films with water/propylene carbonate/surfactant mixtures – implications for cultural heritage conservation. Phys Chem Chem Phys. 2017;19:23723–32.

19. Baglioni M, Montis C, Chelazzi D, Giorgi R, Berti D, Baglioni P. Polymer Film Dewetting by Water/Surfactant/Good-Solvent Mixtures: A Mechanistic Insight and Its Implications for the Conservation of Cultural Heritage. Angew Chem Int Ed. 2018;57:7355–9.

20. Baglioni M, Alterini M, Chelazzi D, Giorgi R, Baglioni P. Removing Polymeric Coatings With Nanostructured Fluids: Influence of Substrate, Nature of the Film, and Application Methodology. Front Mater [Internet]. 2019 [cited 2019 Dec 10];6. Available from: https://www.frontiersin.org/articles/10.3389/fmats.2019.00311/full

21. Montis C, Koynov K, Best A, Baglioni M, Butt H-J, Berti D, et al. Surfactants Mediate the Dewetting of Acrylic Polymer Films Commonly Applied to Works of Art. ACS Appl Mater Interfaces. 2019;11:27288–96.

22. Baglioni M, Bartoletti A, Bozec L, Chelazzi D, Giorgi R, Odlyha M, et al. Nanomaterials for the cleaning and pH adjustment of vegetable-tanned leather. Appl Phys A. 2016;122:114.

23. Bonelli N, Poggi G, Chelazzi D, Giorgi R, Baglioni P. Poly(vinyl alcohol)/poly(vinyl pyrrolidone) hydrogels for the cleaning of art. J Colloid Interface Sci. 2019;536:339–48.

24. Bonelli N, Chelazzi D, Baglioni M, Giorgi R, Baglioni P. Confined Aqueous Media for the Cleaning of Cultural Heritage: Innovative Gels and Amphiphile-Based Nanofluids. In: Dillmann P, Bellot-Gurlet L, Nenner I, editors. Nanosci Cult Herit [Internet]. Atlantis Press; 2016 [cited 2016 Sep 27]. p. 283–311. Available from: http://link.springer.com/chapter/10.2991/978-94-6239-198-7_10

25. Baglioni M, Domingues JAL, Carretti E, Fratini E, Chelazzi D, Giorgi R, et al. Complex Fluids Confined into Semi-interpenetrated Chemical Hydrogels for the Cleaning of Classic Art: A Rheological and SAXS Study. ACS Appl Mater Interfaces [Internet]. 2018 [cited 2018 Jun 1]; Available from: http://pubs.acs.org/doi/10.1021/acsami.8b01841

26. Baglioni P, Berti D, Bonini M, Carretti E, Del Carmen Casas Perez M, Chelazzi D, et al. Gels for the Conservation of Cultural Heritage. MRS Online Proc Libr. 2012;1418:null-null.

27. Baglioni P, Carretti E, Chelazzi D. Nanomaterials in art conservation. Nat Nanotechnol. 2015;10:287–90.

28. Bonelli N, Montis C, Mirabile A, Berti D, Baglioni P. Restoration of paper artworks with microemulsions confined in hydrogels for safe and efficient removal of adhesive tapes. Proc Natl Acad Sci. 2018;115:5932–7.

29. Mastrangelo R, Montis C, Bonelli N, Tempesti P, Baglioni P. Surface cleaning of artworks: structure and dynamics of nanostructured fluids confined in polymeric hydrogel networks. Phys Chem Chem Phys [Internet]. 2017 [cited 2017 Jul 10]; Available from: http://pubs.rsc.org/en/content/articlelanding/2017/cp/c7cp02662e

30. Giorgi R, Baglioni M, Baglioni P. Nanofluids and chemical highly retentive hydrogels for controlled and selective removal of overpaintings and undesired graffiti from street art. Anal Bioanal Chem. 2017;1–6.

31. Watherston M. Conservation paper stored at The Winterthur Library, Winterthur, Delaware, USA. (Further information available at: http://findingaid.winterthur.org/html/HTML_finding_Aids/col0935.htm).

32. Verschueren K. Handbook of environmental data on organic chemicals. Wiley; 2001.

33. Montis C, Maiolo D, Alessandri I, Bergese P, Berti D. Interaction of nanoparticles with lipid membranes: a multiscale perspective. Nanoscale. 2014;6:6452–7.

34. Ries J, Schwille P. Fluorescence correlation spectroscopy. BioEssays. 2012;34:361–8.

35. Milani S, Baldelli Bombelli F, Pitek AS, Dawson KA, Rädler J. Reversible versus Irreversible Binding of Transferrin to Polystyrene Nanoparticles: Soft and Hard Corona. ACS Nano. 2012;6:2532–41.

36. Bartoletti A, Barker R, Chelazzi D, Bonelli N, Baglioni P, Lee J, et al. Reviving WHAAM! a comparative evaluation of cleaning systems for the conservation treatment of Roy Lichtenstein's iconic painting. Herit Sci. 2020;8:9.

37. Bartoletti A, Maor T, Chelazzi D, Bonelli N, Baglioni P, Angelova LV, et al. Facilitating the conservation treatment of Eva Hesse's Addendum through practice-based research, including a comparative evaluation of novel cleaning systems. Herit Sci [Internet]. 2020 [cited 2020 Apr 17];8. Available from: https://heritagesciencejournal.springeropen.com/articles/10.1186/s40494-020-00378-z

38. Sadaghiania AS, Khan A. Clouding of a nonionic surfactant: The effect of added surfactants on the cloud point. J Colloid Interface Sci. 1991;144:191–200.

39. Nilsson PG, Lindman B. Mixed micelles of nonionic and ionic surfactants. A nuclear magnetic resonance self-diffusion and proton relaxation study. J Phys Chem. 1984;88:5391–7.

40. Valaulikar BS, Manohar C. The mechanism of clouding in triton X-100: The effect of additives. J Colloid Interface Sci. 1985;108:403–6.

41. Gu T, Qin S, Ma C. The effect of electrolytes on the cloud point of mixed solutions of ionic and nonionic surfactants. J Colloid Interface Sci. 1989;127:586–8.

42. Sheu EY, Chen SH. Thermodynamic analysis of polydispersity in ionic micellar systems and its effect on small-angle neutron scattering data treatment. J Phys Chem. 1988;92:4466–74.

43. Liu YC, Ku CY, LoNostro P, Chen SH. Ion correlations in a micellar solution studied by small-angle neutron and x-ray scattering. Phys Rev E. 1995;51:4598–607.

44. Kline SR. Reduction and analysis of SANS and USANS data using IGOR Pro. J Appl Crystallogr. 2006;39:895–900.

45. Degiorgio V, Corti M, fisica S italiana di. Physics of amphiphiles--micelles, vesicles, and microemulsions: Varenna on Lake Como, Villa Monastero, 19-29 July 1983. North-Holland; 1985.

46. Tanford C. The Hydrophobic Effect: Formation of Micelles and Biological Membranes. 2nd edition. New York: Wiley; 1980.

47. Watarai H. Microemulsions in separation sciences. J Chromatogr A. 1997;780:93–102.

48. Eriksson JC, Ljunggren S. Thermodynamic Evaluation of the Polydispersity of Droplet Microemulsions. Langmuir. American Chemical Society; 1995;11:1145–53.

49. Baglioni M, Raudino M, Berti D, Keiderling U, Bordes R, Holmberg K, et al. Nanostructured fluids from degradable nonionic surfactants for the cleaning of works of art from polymer contaminants. Soft Matter. 2014;10:6798–809.

50. Baglioni M, Poggi G, Ciolli G, Fratini E, Giorgi R, Baglioni P. A Triton X-100-Based Microemulsion for the Removal of Hydrophobic Materials from Works of Art: SAXS Characterization and Application. Materials. 2018;11:1144.

51. Mallam S, Horkay F, Hecht AM, Rennie AR, Geissler E. Microscopic and macroscopic thermodynamic observations in swollen poly(dimethylsiloxane) networks. Macromolecules. 1991;24:543–8.

52. Shibayama M, Tanaka T, Han CC. Small angle neutron scattering study on poly(N-isopropyl acrylamide) gels near their volume-phase transition temperature. J Chem Phys. 1992;97:6829–41.

53. Hudson SD, Hutter JL, Nieh M-P, Pencer J, Millon LE, Wan W. Characterization of anisotropic poly(vinyl alcohol) hydrogel by small- and ultra-small-angle neutron scattering. J Chem Phys. 2009;130:034903.

54. Shibayama M, Kurokawa H, Nomura S, Muthukumar M, Stein RS, Roy S. Small-angle neutron scattering from poly(vinyl alcohol)-borate gels. Polymer. 1992;33:2883–90.

55. Lozinsky VI, Damshkaln LG, Kurochkin IN, Kurochkin II. Study of Cryostructuring of Polymer Systems: 25. The Influence of Surfactants on the Properties and Structure of Gas-Filled (Foamed) Poly(vinyl alcohol) Cryogels. Colloid J. 2005;67:589–601.

56. Caykara T, Kiper S, Demirel G. Thermosensitive poly(N-isopropylacrylamide-co-acrylamide) hydrogels: Synthesis, swelling and interaction with ionic surfactants. Eur Polym J. 2006;42:348–55.

57. Chan KLA, Kazarian SG. Detection of trace materials with Fourier transform infrared spectroscopy using a multi-channel detector. Analyst. 2006;131:126–31.